

Electric Cell–Substrate Impedance Sensing (ECIS) as a Noninvasive Means to Monitor the Kinetics of Cell Spreading to Artificial Surfaces

Joachim Wegener, Charles R. Keese, and Ivar Giaever¹

Rensselaer Polytechnic Institute, School of Science, Troy, New York 12180-3590

This article describes the optimization of an experimental technique referred to as electric cell–substrate impedance sensing (ECIS) to monitor attachment and spreading of mammalian cells quantitatively and in real time. The method is based on measuring changes in AC impedance of small gold-film electrodes deposited on a culture dish and used as growth substrate. Based on experimental data and theoretical considerations we demonstrate that high-frequency capacitance measurements ($f = 40$ kHz) are most suited to follow the increasing surface coverage of the electrode due to cell spreading. The excellent time resolution of the method allowed an in-depth analysis of cell spreading kinetics under various experimental conditions. Using ECIS we studied the attachment and spreading of epithelial MDCK cells (strain II) on different protein coatings, and investigated the influence of divalent cations on spreading kinetics. We quantified the inhibitory effect of soluble peptides that mimic the recognition sequence of fibronectin and other extracellular matrix proteins (RGDS). We also applied the ECIS technique to monitor the detachment of confluent fibroblastic cell layers (WI38/VA-13) by means of these peptides. © 2000 Academic Press

Key Words: electric cell–substrate impedance sensing; ECIS; cell adhesion; cell attachment; cell spreading; extracellular matrix; RGDS; real time cell monitoring; biosensor.

INTRODUCTION

The interaction of mammalian cells with artificial surfaces is interesting for both scientific and medical reasons. *In vitro* studies of processes like tumor metastasis, wound healing, or cell migration in general focus on the stationary and dynamic interactions of cultured cells with a particular substrate [1, 2]. The importance of extracellular matrix (ECM) proteins for tissue architecture and integrity, as well as for cell differentiation, has been demonstrated by isolating and studying the

influence of these proteins on cellular behavior when immobilized on a culture substrate. Even in more technical fields, like the development and modification of biomaterials for anatomical implants [3] or the construction of cell–semiconductor interfaces [4], cell attachment is an important parameter. Accordingly, experimental means to monitor the attachment and spreading of animal cells to artificial surfaces are most valuable.

A rather limited number of experimental methods exist that are capable of investigating cell–substrate interactions in a quantitative way. Most techniques impose a mechanical force to the anchored cells and quantify the number of cells resisting this discriminating force and thus remaining attached to the substrate. The forces are applied by means of a centrifugal acceleration [5, 6] or exposure of the cells to laminar shear flow [7]. In the most commonly used cell attachment assay, cells are first seeded onto a substrate. After a certain time interval, weakly adhering cells are rinsed off with a stream of buffer, and the remaining cells are quantified either by counting or by indirect colorimetric assays. More sophisticated methods measure the forces necessary to detach single cells from a given substrate with a force microscope [8] or determine the forces that cells exert on a flexible substrate at oil/water interfaces [9]. Concomitant with cell attachment, complex processes are initiated as cells interact with the substratum to achieve a spread morphology. These events can be quantified by microscopic or ultrastructural techniques often coupled with image analysis. The method described in this article senses the spreading of animal cells upon artificial surfaces in real time and focuses on the kinetic aspects of this phenomenon. It is based on an established technique commonly referred to as electric cell–substrate impedance sensing (ECIS) [10–12]. ECIS uses small gold-film electrodes (diam 250 μm) deposited on the bottom of cell culture dishes and measures the electrode impedance. As the cells attach and spread on the electrode surface, the impedance is altered, and the change can be used to analyze the cell behavior [10]. We have optimized the existing ECIS method in order to follow

¹To whom reprint requests should be addressed. E-mail: giaevi@rpi.edu. Fax: 518-276-2825.

the spreading of animal cells with improved sensitivity, and here we demonstrate its usefulness with several examples that are frequently addressed in cell adhesion studies. Since it has been shown previously that cells anchor essentially in the same way to the gold-film electrodes as they do to normal culture dishes made from treated polystyrene, results extracted from ECIS data are both relevant and significant [13].

Using ECIS we examined the spreading characteristics of the epithelial cell line MDCK when the electrodes were coated with different proteins. We demonstrate the modification of a nonadhesive substrate by the cells, study the effects of the presence and absence of divalent cations (Mg, Ca), and quantify the dose-dependent influence of soluble synthetic peptides (RGDS) that mimic the recognition site of fibronectin and other extracellular matrix proteins. In contrast to other methods used for cell adhesion studies, ECIS can follow the cell behavior continuously and noninvasively for hours, so that certain long-term characteristics of cell attachment and spreading are accessible that have not been considered in traditional assays.

MATERIALS AND METHODS

Instrumentation. The ECIS device is based on AC impedance measurements using weak and noninvasive AC signals as described in more detail elsewhere [14, 15]. Attachment and spreading of cells on the electrode surface change the impedance in such a way that morphological information of the attached cells can be inferred. The measurement system consists of an eight-well cell culture dish with electrodes deposited upon the bottom of each well, a lock-in amplifier with an internal oscillator, relays to switch between the different wells, and a personal computer that controls the measurement and stores the data. The entire system was obtained from Applied BioPhysics, Inc. (Troy, NY 12180, <http://www.biophysics.com>) and is schematically depicted in Fig. 1.

The oscillator applies an AC signal of amplitude 1 V through a series 1 Mohm. resistor to the two-electrode system. With this setup and using culture medium as the electrolyte, the current flow is approximately constant at 1 μ A. The in-phase and out-of-phase voltages across the system are measured by the amplifier and converted to real and imaginary components of the electrode impedance, which are presented formally as resistance and capacitance of a RC series circuit. We acquired data as a function of time in two different ways: (i) In the frequency scan mode, the impedance is measured at 23 different frequencies between 10 and 10^5 Hz. (ii) In most experiments, however, we followed the impedance of the system at only 3 frequencies, namely 400 Hz, 4 kHz, and 40 kHz. This measuring mode provided better time resolution while still providing data for the most important frequency ranges.

Electrode arrays. Each electrode well contains a small working electrode (area = $5 \cdot 10^{-4}$ cm²) and a large counter electrode (area = 0.15 cm²). Due to the difference in surface area (~300-fold), the total impedance of the system is determined mainly by the impedance of the small electrode. In addition to this there is a frequency-independent series resistance of roughly 900 ohm due to the solution resistance, especially that immediately next to the small electrode (constriction resistance) as well as a small amount due to leads and contacts. Prior to cell inoculation the electrode arrays were treated in an oxygen-plasma for 60 s, providing both an intense cleaning of the electrodes and sterilization of the entire array. Directly after plasma

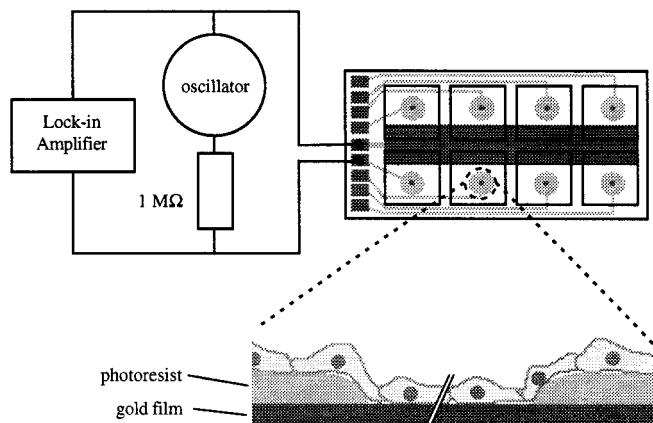


FIG. 1. Schematic of the experimental setup to perform electric cell-substrate impedance sensing. Details are given under Materials and Methods. The active electrode area is delineated by circular openings ($\varnothing = 250 \mu\text{m}$) in a photoresist overlayer that insulates the rest of the deposited gold from the bulk electrolyte. Note that the size of the electrode in the magnified presentation is not drawn to scale with respect to cell size.

etching, the electrodes were immersed with an aqueous solution of 10 mM L-cysteine (Sigma), which binds to the gold surface via its thiol group forming a monomolecular layer [16]. We found that this procedure resulted in improved reproducibility of the electrode/electrolyte interface impedance. In experiments in which cell adhesion to a protein-coated surface was studied, we flooded the electrode with a 100 μ g/ml solution of the particular protein in saline (0.15 M NaCl in water) for 75 min at room temperature. Afterward, electrodes were thoroughly washed with three rinses of serum-free medium to remove nonadherent protein.

Cell culture. This study includes experiments with the epithelial cell line MDCK (strain II) derived from canine kidney and the fibroblastic cell line WI38/VA-13 transformed from human embryonic lung fibroblasts. Both cell types were kept in an ordinary humidified cell culture incubator at 37°C and 5% CO₂ (v/v) and were treated identically. We used Dulbecco's modified Eagle's medium (DMEM) with 1 g/L glucose (Sigma, St. Louis) as basic medium supplemented with 10% (v/v) fetal calf serum (Sigma) and 50 μ g/ml gentamicin. The culture medium was exchanged twice a week, and routine subculturing of confluent cell layers was performed using standard trypsinization (0.05% (w/v)/1.5 mM EDTA) techniques.

Cell attachment/spreading assay. Suspensions of MDCK cells for inoculation of ECIS electrodes were routinely prepared from confluent cell layers by first washing the cells with phosphate-buffered saline without divalent cations (PBS). Cell layers were then incubated with PBS supplemented with 1 mM EDTA (Sigma) for 10 min at 37°C followed by a 10-min treatment with 0.05% (w/v) trypsin in presence of 1.5 mM EDTA. Trypsinization was terminated by adding an excess of complete culture medium. Cells were spun down at 100g for 10 min and were then resuspended in serum-free culture medium. The cell density was monitored using a standard hemacytometer, and the inoculum was adjusted to give a final cell density between 4×10^5 and 5×10^5 cells/cm². Prior to inoculation ECIS electrodes were equilibrated with a small amount of serum-free medium under incubator conditions. In experiments using the integrin-blocking peptide Arg-Gly-Asp-Ser (RGDS, Sigma) appropriate volumes of the peptide stock solutions (in PBS) were added to the electrode-containing wells before cells were seeded. In vehicle control experiments, only PBS was added to the medium.

Cell detachment assay. We also used ECIS to monitor the effect of the RGDS tetrapeptide on cell-substrate adhesion of already estab-

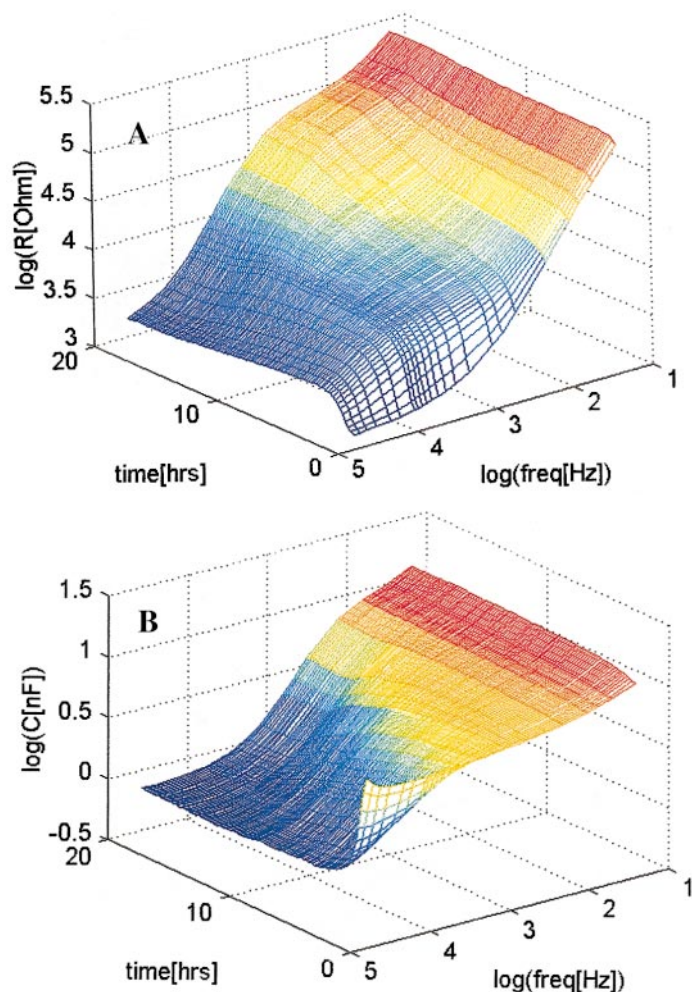


FIG. 2. Three-dimensional representation of the changes in resistance (A) and capacitance (B) as a function of frequency and time during the attachment and spreading of MDCK cells on ECIS electrodes. In this experiment serum-containing culture medium was used and the electrodes were not precoated with protein.

lished WI38/VA-13 cell layers and to follow cell detachment from the substrate. In these experiments cells were grown to confluence in the electrode wells and confluence was verified both microscopically and via ECIS measurements. After baseline recordings, the peptide or the corresponding vehicle control (PBS) was added to the electrode wells, and the cell response was monitored as a function of time.

RESULTS AND DISCUSSION

We first followed the resistance and capacitance of the ECIS electrodes during the attachment of initially suspended MDCK cells over the entire frequency range (10 to 10^5 Hz) in order to determine the most relevant and sensitive frequencies. Figs. 2A and 2B shows a three-dimensional representation of continuously recorded frequency scans. The cells were seeded into the electrode array at time zero using serum-containing

medium and were followed for 20 h. The measured resistance (Fig. 2A) at the low-frequency ($f < 75$ Hz) end of the spectrum is very insensitive to the spreading of the cells on the electrode surface, as it is dominated by the rather high resistance of the electrode/electrolyte interface at these frequencies. Looking at intermediate frequencies ($200 \text{ Hz} < f < 5 \text{ kHz}$), the resistance seems to have a biphasic time course. It increases from values of the naked electrode shortly after inoculation, goes through a period of slow increase, and then rises to its final values. We will show below that only the initial increase of the resistance is due to attachment and spreading of the cells, whereas the later changes ($t > 10$ h) reflect the establishment of tight intercellular contacts, so-called tight junctions, that restrict the current flow between neighboring cells. The high-frequency resistance ($f > 10 \text{ kHz}$) shows an immediate but rather small increase and starts to slowly decline after 2 h. The characteristics of the measured capacitance (Fig. 2B) are less involved. At the low-frequency end of the spectrum ($f < 200 \text{ Hz}$) the measured capacitance is fairly invariant at all times. When moving to higher frequencies the measurements get continuously more sensitive to the changes at the electrode surface due to cell attachment and spreading. Recent studies show that MDCK cells attach and spread upon an artificial substrate within the first 2 to 3 h after seeding [17], suggesting that the high-frequency capacitance is the most sensitive parameter for monitoring the early events during establishment of a cell layer. In contrast to resistance measurements at most frequencies, high-frequency capacitance readings are barely ($< 10\%$) affected by the subsequent formation of intercellular junctions between adjacent MDCK cells.

Another important feature associated with high-frequency capacitance measurements becomes obvious from theoretical consideration. As sketched in Fig. 3, the cells reach the substrate with an almost spherical morphology. The area of closest contact between basal membrane and surface is therefore rather small but increases continuously while the cells spread. Since the cell membrane is essentially insulating and restricts current flow, current leaving the electrode in the adhesion area has to flow in the narrow channels underneath the cells before it can escape in the bulk electro-

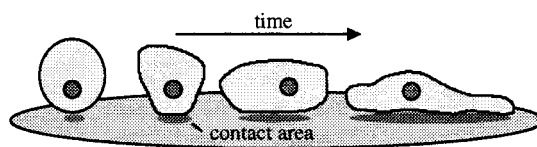


FIG. 3. Time course of cell spreading on a culture substrate and the concomitant increase of the adhesion area's projection on the substrate.

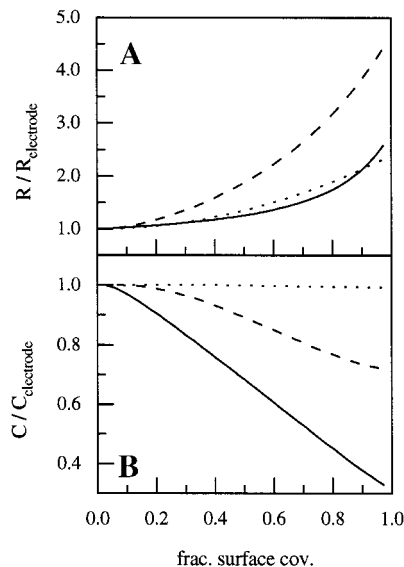


FIG. 4. Calculated resistance (A) and capacitance (B) values of ECIS electrodes as a function of fractional coverage of the surface with adherent cells. Electrode parameters were modeled for three different frequencies as detailed in the text: (\cdots) 400 Hz, ($---$) 4 kHz, ($-$) 40 kHz. For better comparison both quantities are normalized to the corresponding values of a naked electrode.

lyte at the cell perimeter. Current flow within the adhesion area is furthermore dependent on the applied frequency. We modeled this situation at the electrode surface by calculating the evolution of resistance and capacitance values as a function of surface coverage for the three major measuring frequencies (400 Hz, 4 kHz, 40 kHz). The calculation is based on a published model [11] that predicts the impedance of a cell-covered electrode from morphological parameters of the respective cells. In this model the cells are described as circular disks of radius r_c that are spaced an average distance h above the gold surface. The impedance of the cell-covered electrode is then dependent on the impedance of the electrode itself, the resistance between adjacent cells R_b , the capacitance of the cell membrane C_m , and a parameter α . The α term describes the impedance contributions arising from current flow in the adhesion area and is given by $\alpha = r_c \cdot (\rho/h)^{1/2}$. It depends on the average distance between basal plasma membrane and substrate h , the specific resistivity of the medium in the cleft ρ and the radius of the spread cell r_c . Here we apply the model to the special case that there is no resistance between adjacent cells ($R_b = 0$). To keep the calculation simple we considered only the area of closest contact and assumed it to be circular with an average distance between membrane and substrate of $h = 10$ nm. The capacitance of the cell membrane C_m was set to $1 \mu\text{F}/\text{cm}^2$ and the radius of the entirely spread cells r_c was set to $7.5 \mu\text{m}$, as has been reported for MDCK-II cells previously [17]. Figures 4A and 4B sum-

marize the result of the calculation for the measuring frequencies 400 Hz, 4 kHz, and 40 kHz. For better comparison, resistance and capacitance values were divided by the respective values of the naked electrode and are now referred to as normalized resistance and capacitance. In excellent agreement with the measured data shown in Fig. 2, the calculation confirms the large change in resistance for the intermediate frequency and the large change in capacitance for the high frequency. Note, however, that since the measured capacitance at 40 kHz (Fig. 4B) decreases approximately linearly with increasing surface coverage, it is well suited to serve as a direct measure for the degree of cell spreading on the electrode surface.

After these more general considerations about the measurement, we will demonstrate its applicability to typical questions that arise in the context of cell adhesion to culture substrates. Figure 5 shows the time course of the capacitance measured at 40 kHz when MDCK-II cells suspended in serum-free medium were seeded into the measuring arrays. In this experiment the electrodes were precoated with various proteins, as given in the figure caption. The time course of the measured capacitance mirrors the attachment and spreading of MDCK cells to the different protein coatings with a time resolution of less than 3 min. In order to describe the individual spreading behavior we extracted two quantities from the measured time courses: (i) We determined the time ($t_{1/2}$) necessary to produce a half-maximum capacitance decrease as indicated in Fig. 5 for the laminin-coated electrode. According to

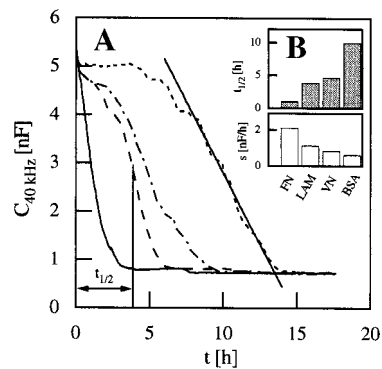


FIG. 5. (A) Time courses of the capacitance measured at 40 kHz when MDCK cells are seeded into ECIS arrays whose electrodes were coated with different proteins: fibronectin (FN) ($-$); laminin (LAM) ($---$); vitronectin (VN) ($- \cdot -$); bovine serum albumin (BSA) (\cdots). We extracted two quantities from the respective time courses that are useful to describe cell spreading on a particular protein. $t_{1/2}$ denotes the time necessary to achieve half-maximum capacitance drop as it is indicated in the figure for the laminin-coated electrode. The slope of the curve s between $C = 4$ nF and $C = 2$ nF—equivalent to the apparent rate of spreading—was extracted from this data range by linear regression as shown for the BSA-coated electrode. (B) Half-times $t_{1/2}$ and apparent spreading rates s as determined from the data shown in (A).

the preceding paragraph $t_{1/2}$ should correspond to the time required for the cells to spread out on half (50%) the available electrode area. (ii) We determined the average slope of the capacitance shift ($s = -\Delta C/\Delta t$) between $C = 4$ nF and $C = 2$ nF by means of linear regression as indicated in Fig. 5 for the bovine serum albumin (BSA)-coated electrode. The term s then corresponds to the rate of cell spreading. We chose this range of capacitance data for analysis, as it more or less symmetrically embraces the capacitance values at $t = t_{1/2}$. In the typical example shown in Fig. 5 we determined half-times $t_{1/2}$ of 1.0 h for fibronectin (FN), 3.8 h for laminin (LAM), 4.6 h for vitronectin (VN), and 10.0 h for BSA. The apparent spreading rates s were quantified to 2.1 nF/h for FN, 1.1 nF/h for LAM, 0.8 nF/h for VN, and 0.6 nF/h for BSA. Results are compared in Fig. 5B. MDCK cells spread significantly faster on FN-coated substrates than on any of the other proteins examined. Although it was not the objective of this study to deduce information about the expression of certain integrins in MDCK cells, it is interesting to compare the results shown in Fig. 5 with published data. More recent studies [18, 19] identified several integrins that are expressed on the MDCK cell surface. Among those are two possible FN receptors ($\alpha_3\beta_1$, $\alpha_v\beta_3$) and two possible VN receptors ($\alpha_v\beta_5$, $\alpha_v\beta_3$) [20]. The authors [18] concluded from experimental evidence that attachment to FN and VN were likely to be mediated by the same integrin $\alpha_v\beta_3$. If this conclusion applies, our ECIS data suggest that the $\alpha_v\beta_3$ integrin has very different affinities toward these two proteins, as we found that the spreading behavior for the two pro-

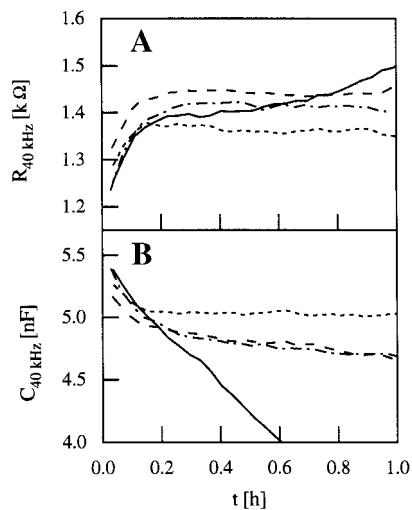


FIG. 6. Magnified presentation of resistance and capacitance changes at 40 kHz during the first hour of the experiment shown in Fig. 5: FN (—); LAM (---); VN (- · -); BSA (· · ·). Note the immediate increase of the resistance and the corresponding decrease of the capacitance, which are due to the settlement of the cells to the electrode surface.

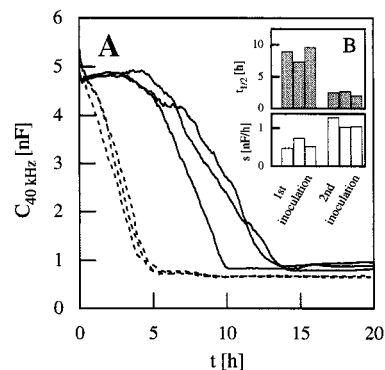


FIG. 7. (A) Time course of the capacitance measured at 40 kHz when MDCK cells are seeded into ECIS arrays whose electrodes were coated with BSA (—). After 24 h these cells were gently removed from the surface and a fresh cell suspension was seeded on the same electrodes (- · -). Serum-free medium was used in both cases. (B) Half-times $t_{1/2}$ and apparent spreading rates s as determined from the data shown in (A).

tein coatings were rather different (Fig. 5). However, MDCK cells examined in that particular study showed less efficient attachment to FN-coated substrates compared to LAM or VN within 90 min after seeding, whereas we consistently observed the fastest attachment and spreading for FN coatings.

Figures 6A and 6B provide a more detailed view on the changes of resistance and capacitance at the very beginning ($t < 1$ h) of the experiment shown in Fig. 5. The capacitance decreases immediately after cell seeding in the order of 0.5 nF, and the resistance increases by 150 to 200 ohm. From experiments with electrode arrays in which we extended the sedimentation pathways for the suspended cells (data not shown), we learned that these initial changes of the parameters are due to the settling of the cells onto the electrode surface. As these changes also occur when integrin-mediated cell adhesion is experimentally omitted (see below), we conclude that loose attachment or even the sole presence of the cellular bodies close to the electrode surface is detectable by ECIS.

The time course of the measured capacitance for BSA-coated electrodes is interesting. According to the data depicted in Fig. 5, it takes more than 5 h before MDCK cells start to spread on a BSA-coated substrate; furthermore, the slope of the curve reveals that the spreading rate is considerably smaller than for FN- or LAM-coated electrodes. It is quite likely that the cells need the delay time in order to modify the nonadhesive BSA substrate by secreting self-produced extracellular matrix proteins. Accordingly, we tried to demonstrate this phenomenon by using ECIS. Figure 7A (—) shows the time course of the high-frequency capacitance when three electrodes coated with 200 $\mu\text{g/ml}$ BSA were inoculated with a suspension of MDCK cells in serum-free medium. The measured time courses are very sim-

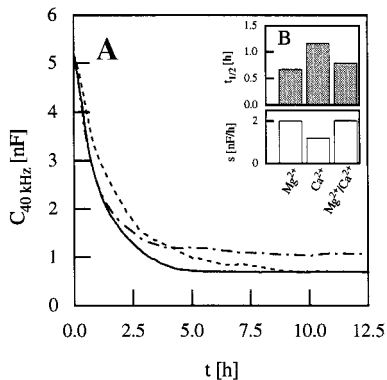


FIG. 8. (A) Time course of the capacitance measured at 40 kHz when MDCK cells were seeded into ECIS arrays whose electrodes were coated with fibronectin. The cell suspension was prepared in Earles' balanced salt solution with Ca^{2+} and Mg^{2+} (—); Mg^{2+} only (- · -), or Ca^{2+} (- - -) only. (B) Half-times $t_{1/2}$ and apparent spreading rates s as determined from the data shown in (A).

ilar to the one shown in Fig. 5 ($t_{1/2} = 7.3 - 9.6$ h; $s = 0.48 - 0.73$ nF/h). Twenty-four hours after seeding, these cells were removed from the electrode surface by 1 mM EDTA in phosphate-buffered saline and very gentle trypsinization. The electrodes were extensively washed and then inoculated with a fresh suspension of MDCK cells in serum-free medium. The time course of the capacitance under these conditions is given in the same figure (- - -). It is obvious that MDCK cells now attach and spread on the electrodes much faster ($t_{1/2} = 2.0 - 2.7$ h; $s = 1.0 - 1.3$ nF/h). With no exogenous protein deposition involved, the initially seeded cells must have modified the substrate with adhesion-promoting proteins. This is consistent with previous reports [21] in which it was shown that MDCK cells produce and secrete endogenous LAM upon their culture substrate and that the endogenous LAM is essential for the development of the polarized epithelial phenotype [22]. Comparison of the characteristic half-times $t_{1/2}$ and spreading rates s for the second inoculation (Fig. 7B) with the data recorded for a LAM-coated electrode (Fig. 5B) agrees with a potential LAM deposition on the electrode surface.

Integrins, which are mainly responsible for attachment and spreading of animal cells, require divalent cations in the extracellular medium to bind to their recognition sites on the ECM proteins. Different integrin subtypes show different preferences for Ca^{2+} or Mg^{2+} , and some are even inhibited by the other ionic species [23]. Thus, we studied the time course of attachment and spreading of MDCK cells on FN-coated electrodes, when either Ca^{2+} or Mg^{2+} or both were present in the serum-free salt solution during cell attachment and spreading; results are depicted in Fig. 8. As a linear approximation of the recorded capacitance data was only meaningful for values between 3.5 and

2.5 nF, the spreading rates in this experiment were determined from data in that interval and are referred to as s' . The time course of the capacitance reveals that MDCK cells spread slightly faster on the FN-coated electrode if Mg^{2+} is present in the extracellular medium either alone ($t_{1/2} = 0.7$ h; $s' = 2.0$ nF/h) or with Ca^{2+} ($t_{1/2} = 0.8$ h; $s' = 2.0$ nF/h). The data recorded in the presence of Ca^{2+} only had a slower time course ($t_{1/2} = 1.2$ h; $s' = 1.2$ nF/h). From these data we can conclude that (i) the integrins responsible for FN binding in MDCK cells show a higher binding affinity for FN in the presence of Mg^{2+} and (ii) that the integrin binding site for divalent cations favors binding of Mg^{2+} , when both cations are present in the concentrations applied here. Based on the common formulations of cell culture media, the buffer solution contained 0.9 mM Mg^{2+} but 1.8 mM Ca^{2+} . The presence of Ca^{2+} , however, causes the capacitance to drop to lower values toward the end of the experiment either alone or in the presence of Mg^{2+} . In order to understand the source of these differences, we performed frequency scan experiments (data not shown) immediately after the measurement depicted in Fig. 8 had been terminated. The result was analyzed with the theoretical model mentioned above. This analysis revealed that the differences in high-frequency capacitance are mainly due to differences in the cell-substrate adhesion parameter α that is $16 \Omega^{1/2} \cdot \text{cm}$ in the presence of Ca^{2+} but $4 \Omega^{1/2} \cdot \text{cm}$ in the absence of Ca^{2+} . According to its definition, these changes in α can be caused either by a corresponding change of the radius of the spread cell (r_c), the average distance between cell layer and substrate (h), the specific resistivity (ρ) in the adhesion zone, or any combination of these. A small contribution to the altered capacitance values at high frequencies is also due to the establishment of tight junctions between adjacent cells. The formation of these barrier forming cell-cell contacts is strictly dependent on the presence of physiological concentrations of Ca^{2+} in the extracellular medium [24]. Accordingly, the analysis of the frequency scan data revealed that the resistance between cells R_b amounts to $30 \Omega \cdot \text{cm}^2$ in the presence of Ca^{2+} but only $0.5 \Omega \cdot \text{cm}^2$ in its absence.

Some of the more than 20 integrin subtypes that have been identified so far bind to extracellular matrix proteins via a common recognition sequence, namely Arg-Gly-Asp-Ser (RGDS) [25, 26]. The RGDS sequence has been found in fibronectin, vitronectin, collagens, laminin, and others [27]. When soluble peptides that contain the RGDS sequence are added to the culture medium, they compete with extracellular matrix proteins for the integrin binding sites and may thereby inhibit normal attachment of cells or even detach already established cell layers [28]. We studied the attachment of suspended MDCK cells to either FN- or LAM-coated ECIS electrodes in the presence of in-

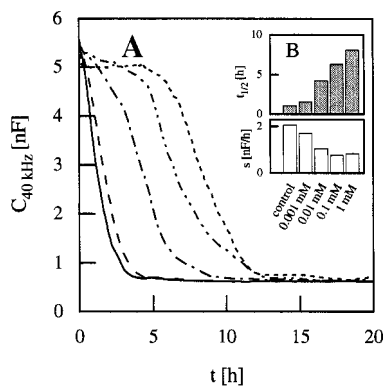


FIG. 9. (A) Time course of the capacitance measured at 40 kHz during attachment and spreading of MDCK cells on fibronectin-coated electrodes in presence of increasing amounts of the synthetic tetrapeptide RGDS: control (—); 0.001 mM (---); 0.01 mM (- · -); 0.1 mM (- - -); 1 mM (· · ·). (B) Half-times $t_{1/2}$ and apparent spreading rates s as determined from the data shown in (A).

creasing amounts of the tetrapeptide RGDS. The results are shown in Fig. 9 for FN and Fig. 10 for LAM. In case of the FN-coated electrode (Fig. 9) increasing concentrations of RGDS in the medium gradually delay the onset of cell spreading on the electrode surface with respect to the control. For the highest concentration applied (1 mM RGDS) we determined $t_{1/2}$ to be 8.1 h compared to $t_{1/2}$ of 1.1 h under control conditions. Not only the onset of cell spreading is considerably delayed, but also the presence of the peptide is reflected in the apparent spreading rates that decrease from $s = 2.1$ nF/h under control conditions to $s = 0.8$ nF/h in presence of 1 mM RGDS. Results are summarized in Fig. 9B, where dose dependency of RGDS inhibition is apparent.

The corresponding experiment showed somewhat different results when LAM-coated electrodes were

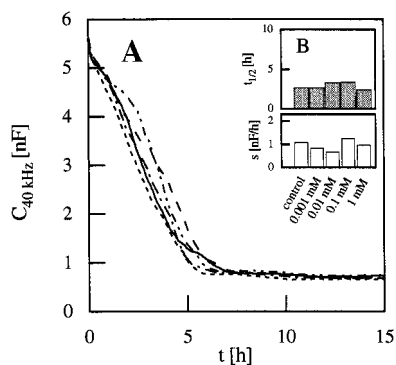


FIG. 10. (A) Time course of the capacitance measured at 40 kHz during attachment and spreading of MDCK cells on laminin-coated electrodes in presence of increasing amounts of the synthetic tetrapeptide RGDS: control (—); 0.001 mM (---); 0.01 mM (- · -); 0.1 mM (- - -); 1 mM (· · ·). (B) Half-times $t_{1/2}$ and apparent spreading rates s as determined from the data shown in (A).

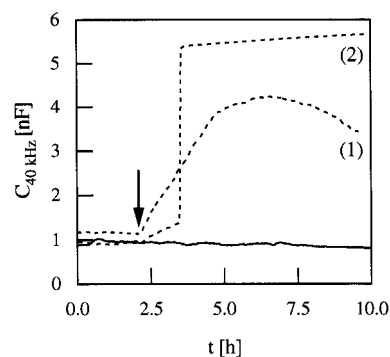


FIG. 11. Time course of the capacitance at 40 kHz when confluent WI38/VA-13 cells were treated with 1 mM RGDS (---) [(1) and (2)] or a corresponding vehicle control (—). Addition of the peptide is indicated by an arrow.

used (Fig. 10). In this case, increasing amounts of RGDS present in the medium did not delay the onset of cell spreading in the manner observed for FN-coated electrodes. The range of characteristic spreading times $t_{1/2}$ ($t_{1/2} = 2.4$ – 3.4 h) was very similar to the range of values we obtained when all attachment experiments to LAM-coated electrodes in serum-free medium (control conditions) were pooled. The presence of RGDS in the medium did not have any significant influence on the apparent spreading rates as well (Fig. 10B). As soluble RGDS peptides cannot interfere with MDCK attachment and spreading on LAM, it is reasonable to conclude that anchorage of MDCK cells to LAM is mediated by receptor–ligand interactions that do not use the RGDS recognition sequence. Several previous reports have shown similarly that cell attachment to laminin may not depend on an RGDS-based mechanism [29], despite the fact that there is a RGD site present in LAM [30]. In particular for MDCK cells of strain II, which were used in this study, it has been shown that anchorage of these cells to LAM is not necessarily mediated by integrins or other protein receptors, but is rather accomplished by a glycolipid, the so-called Forssman antigen [22].

We also applied the ECIS technology to monitor the interference of soluble RGDS peptides with already established cell layers. In order to allow the tetrapeptide to diffuse to cell–substrate attachment sites, we did not utilize the barrier-forming MDCK cells in these experiments, but performed experiments with the transformed fibroblastic cell line WI38/VA-13. Figure 11 shows the result of two typical experiments when confluent WI38/VA-13 cells were treated with 1 mM RGDS or with the corresponding vehicle control. The data demonstrate the different ways in which the cell layers responded in our hands to peptide addition. In trace (1), the high-frequency capacitance rises smoothly from its starting value of 1.2 nF to a maximum of 4.2 nF and then gradually recovers. The RGDS

peptide apparently interfered considerably with the adhesion of the cells to the electrode but did not entirely detach them. In trace (2), however, the capacitance increases slowly at first but then abruptly changes to values that we typically record for naked electrodes. Microscopic inspection revealed that the cell layer as a whole was rolled up and removed from the culture substrate, indicating the integrity of cell-cell contacts. Thus far, we do not understand the reasons for these differences, but we made similar observations when the murine fibroblastic cell line NIH-3T3 was used in the experiment. The control experiment, however, did not show any significant changes that could be associated with mechanical disturbances due to the addition of fluid into the electrode well. Hayman *et al.* [28] reported on detachment experiments with NRK cells, in which the effect of RGDS-related peptides was to some degree dependent on the age and density of the culture. A similar mechanism may also apply to our data but we did not examine this particular relationship.

The data presented in this article demonstrate that electric cell-substrate impedance sensing is a versatile tool to perform in-depth analysis of various aspects of cell adhesion to artificial surfaces. In particular the capacitance measured at 40 kHz mirrors the attachment and spreading of cells in a linear fashion. The excellent time resolution of the technique together with computer-controlled measurements of up to 16 samples in parallel permits highly quantitative data of cell attachment kinetics in real time. Due to the non-invasive nature of the measurement, even long-term effects of different substrate compositions that have not been considered in traditional assays are accessible.

This work was performed in part pursuant to a contract with the National Foundation for Cancer Research. A scholarship granted to J.W. by the German Academic Exchange Service (DAAD) is gratefully acknowledged.

REFERENCES

1. Lauffenburger, D. A., and Horwitz, A. F. (1996). Cell migration: A physically integrated molecular process. *Cell* **84**, 359–369.
2. Horwitz, A. R., and Parsons, J. T. (1999). Cell migration—Movin' on. *Science* **286**, 1102–1103.
3. Vogler, E. A. (1988). Thermodynamics of short-term cell adhesion in vitro. *Biophys. J.* **53**, 759–769.
4. Parak, W. J., Domke, J., George, M., Kardinal, A., Radmacher, M., Gaub, H. E., de Roos, A. D. G., Theuvenet, A. P. R., Wiegand, G., Sackmann, E., and Behrends, J. C. (1999). Electrically excitable normal rat kidney fibroblasts: A new model for cell-semiconductor hybrids. *Biophys. J.* **76**, 1659–1667.
5. Crouche, C. F., Fowler, H. W., and Spier, R. E. (1985). The adhesion of animal cells to surfaces: The measurement of critical surface shear stress permitting attachment or causing detachment. *J. Chem. Tech. Biotechnol. B* **35**, 273–281.
6. Channavajjala, L. S., Eidsath, A., and Saxinger, W. (1997). *J. Cell Sci.* **110**, 249–256.
7. Xiao, Y., and Truskey, G. A. (1996). Effect of receptor–ligand affinity on the strength of endothelial cell adhesion. *Biophys. J.* **71**, 2869–2884.
8. Sagvolden, G., Giaever, I., Petersen, E. O., and Feder, J. (1999). Cell adhesion force microscopy. *Proc. Natl. Acad. Sci. USA* **96**, 471–476.
9. Keese, C. R., and Giaever, I. (1991). Substrate mechanics and cell spreading. *Exp. Cell Res.* **195**, 528–532.
10. Giaever, I., and Keese, C. R. (1993). A morphological biosensor for mammalian cells. *Nature* **366**, 591–592.
11. Giaever, I., and Keese, C. R. (1991). Micromotion of mammalian cells measured electrically. *Proc. Natl. Acad. Sci. USA* **81**, 3761–3764. *Erratum: Proc. Natl. Acad. Sci. USA* **90** (1993), 1634.
12. Giaever, I., and Keese, C. R. (1986). Use of electric fields to monitor the dynamical aspect of cell behavior in tissue culture. *IEEE Proc. Biomed. Engin.* **33**, 242–247.
13. Mitra, P., Keese, C. R., and Giaever, I. (1991). Electric measurements can be used to monitor the attachment and spreading of cells in tissue culture. *Biotechniques* **11**(4), 504–510.
14. Lo, C. M., Keese, C. R., and Giaever, I. (1995). Impedance analysis of MDCK cells measured by electric cell-substrate impedance sensing. *Biophys. J.* **69**, 2800–2807.
15. Keese, C. R., and Giaever, I. (1994). A biosensor that monitors cell morphology with electric fields. *IEEE Eng. Med. Biol.* **13**, 402–408.
16. Tengvall, P., Lestelius, M., Liedberg, M., and Lundstroem, I. (1992). Plasma protein and antisera interactions with L-cysteine and 3-mercaptopropionic acid monolayers on gold surfaces. *Langmuir* **8**, 1236–1238.
17. Wegener, J., Janshoff, A., and Galla, H.-J. (1998). Cell adhesion monitoring using a quartz crystal microbalance: Comparative analysis of different mammalian cell lines. *Eur. Biophys. J.* **28**, 26–37.
18. Schoenenberger, C. A., Zuk, A., Zinkl, G. M., Kendall, D., and Matlin, K. S. (1994). Integrin expression and localization in normal MDCK cells and transformed MDCK cells lacking apical polarity. *J. Cell Sci.* **107**, 527–541.
19. Ojakian, G. K., and Schwimmer, R. (1994). Regulation of epithelial cell surface polarity reversal by $\beta 1$ integrins. *J. Cell Sci.* **107**, 561–576.
20. Marcantonio, E. E. (1996). The structure and function of integrins *In* “Advances in Molecular and Cell Biology” (E. E. Bittar, Ed.), Vol. 16, pp. 1–29.
21. Salas, P. I. J., Vega-Salas, D. E., and Rodriguez-Boulan, E. (1987). Collagen receptors mediate early events in the attachment of epithelial (MDCK) cells. *J. Membr. Biol.* **98**, 223–236.
22. Zinkl, G. M., Zuk, A., Van der Bijl, P., van Meer, G., and Matlin, K. S. (1996). An antiglycolipid antibody inhibits Madin–Darby canine kidney cell adhesion to laminin and interferes with basolateral polarization and tight junction formation. *J. Cell Biol.* **133**, 695–708.
23. Kirchhofer, D., Grzesiak, J., and Pierschbacher, M. D. (1991). Calcium as a potential physiological regulator of integrin-mediated cell adhesion. *J. Biol. Chem.* **266**(7), 4471–4477.
24. Gonzales-Mariscal, L., Contreras, R. G., Bolivar, J. J., Ponce, A., Chavez de Ramirez, B., and Cerejido, M. (1990). Role of Ca^{2+} in tight junction formation between epithelial cells. *Am. J. Physiol. C* **259**, 978–986.

25. Pierschbacher, M. D., and Ruoslahti, E. (1984). Cell attachment activity of fibronectin can be duplicated by small synthetic fragments of the molecule. *Nature* **309**, 30–33.
26. Ruoslahti, E., and Pierschbacher, M. D. (1987). New perspectives in cell adhesion: RGD and integrins. *Science* **238**, 491–497.
27. Ruoslahti, E. (1991). Integrins as receptors for extracellular matrix. In "Cell Biology of Extracellular Matrix" (E. D. Hay, Ed.), Plenum Press, New York.
28. Hayman, E. G., Pierschbacher, M. D., and Ruoslahti, E. (1985). Detachment of cells from culture substrate by soluble fibronectin fragments. *J. Cell Biol.* **100**, 1948–1954.
29. Pytela, R., Pierschbacher, M. D., and Ruoslahti, E. (1985). Identification and isolation of a 140 kDa cell surface glycoprotein with properties expected of a fibronectin receptor. *Cell* **40**, 191–196.
30. Tashiro, K., Sephel, G. C., Grotorex, D., Sasaki, M., Shirashi, M., Martin, G. R., Kleinman, H. K., and Yamada, Y. (1991). The RGD containing site of the mouse laminin A chain is active for cell attachment, spreading, migration and neurite outgrowth. *J. Cell Physiol.* **146**(3), 451–459.

Received February 15, 2000